[CANCER RESEARCH 62, 1688–1695, March 15, 2002]

Transcriptional Regulation of Mitotic Genes by Camptothecin-induced DNA Damage: Microarray Analysis of Dose- and Time-dependent Effects

Yi Zhou,[1] Fuad G. Gwadry, William C. Reinhold, Lance D. Miller, Lawrence H. Smith, Uwe Scherf, Edison T. Liu, Kurt W. Kohn, Yves Pommier, and John N. Weinstein[2]

Laboratory of Molecular Pharmacology, Division of Basic Sciences [Y. Z., F. G. G., W. C. R., L. H. S., U. S., K. W. K., Y. P., J. N. W.], Microarray Facility, Advanced Technology Center, Division of Clinical Sciences [L. D. M.], and Office of the Director, Division of Clinical Sciences [E. T. L.], National Cancer Institute, NIH, Bethesda, Maryland 20892

ABSTRACT

cDNA microarray technology can be used to establish associations between characteristic gene expression patterns and molecular responses to drug therapy. In this study, we used cDNA microarrays of 1694 cancer-related genes to monitor the gene expression consequences of the treatment of HCT116 colon cancer cells with the topoisomerase I inhibitor camptothecin (CPT). To obtain a more homogeneous cellular response, we synchronized the cells in S-phase using aphidicolin (APH) before CPT treatment. Brief incubation with 20 and 1000 nM CPT caused reversible and irreversible G_2 arrest, respectively, and the patterns of gene expression change (with reference to untreated controls) were strikingly different at the two concentrations. Thirty-three genes, mainly divided into three groups, showed characteristic changes in the first 20 h as a consequence of treatment. Northern blots performed for five of these genes (each under eight experimental conditions) were quite consistent with the microarray results (average correlation coefficient, 0.86). Several p53-activated stress response genes were up-regulated after treatment with 1000 nM CPT or prolonged exposure to APH, but it seemed that the up-regulation did not directly cause cell cycle arrest because the up-regulation induced by prolonged treatment with APH did not prevent cell cycle progression after removal of APH. In contrast, cell cycle-dependent up-regulation of a group of mitosis-related genes was delayed or blocked after CPT treatments. The interrupted up-regulation of this group of genes was directly associated with G_2 arrest. In addition, we observed down-regulation of gene expression in cells that were recovering from cell cycle delay. The observations reported here suggest a fundamental difference at the gene expression level between the molecular mechanism of reversible G_2 delay that follows mild DNA damage and the mechanism of permanent G_2 arrest that follows more extensive DNA damage.

INTRODUCTION

CPT[3] is a DNA topoisomerase I inhibitor that blocks the DNA religation of topoisomerase I cleavage complexes. During DNA replication, the collision between topoisomerase I cleavage complexes and DNA replication forks generates double-strand breaks (1). Therefore, CPT is most potent during DNA replication (2). DNA damage caused by CPT arrests cells in G_2 phase and can trigger rapid apoptosis in certain cell types (3). CPT derivatives are used clinically to treat many types of solid tumors, including colorectal and ovarian carcinomas, but not all cancer cells are equally sensitive to CPT. Although decreased topoisomerase I expression levels and mutations within topoisomerase I can play important roles in CPT resistance (4), evidence indicates that molecular responses to the DNA damage can also contribute to differential CPT sensitivity (5). These responses, including ones related to cell cycle control, DNA repair, and the apoptotic process, can be both cell-type specific and damage specific. It has been shown that the expression levels of p21/WAF1, cyclin B1, bcl-2, and bax change after CPT treatment (6, 7). Transcriptional changes after DNA damage can be either primary responses to the damage or secondary to cellular processes responding to the damage. Identification of changes in gene expression levels can provide a useful link between DNA damage and drug cytotoxicity (8, 9). cDNA microarray technology (10–12) makes it possible to measure changes in the relative expression levels of thousands of genes and, therefore, to study multiple cellular processes simultaneously.

In this study, using pin-spotted cDNA microarrays, we measured relative changes in expression of 1694 genes after brief CPT treatment of HCT116 cells. HCT116 is a MSH-2-deficient, non-apoptotic colon cancer-derived cell line that expresses functional p53 protein (13). HCT116 cells arrest in G_2-M phase after DNA damage, but unlike leukemia cell lines, they do not undergo rapid apoptosis (14). This property was used to separate gene expression changes directly related to DNA damage from those associated with apoptosis. To obtain more homogeneous response to CPT treatment and distinguish changes in gene expression related to cell cycle from changes related to DNA damage, we carried out experiments using HCT116 cells synchronized in S-phase. The synchronization allowed us to discern cell cycle-dependent down-regulation and modest up-regulations that would have been buried in an unsynchronized (mixed) population of cells. By performing time- and dose-dependent experiments, we found that up-regulation of p53-related stress response genes was associated with high-dose CPT treatment or prolonged exposure to APH. In contrast, protracted expression of mitosis-related genes was correlated with cell cycle delay in G_2. These results support the twin propositions that DNA damage can disrupt normal cell cycle-related gene expression and that this disruption may be involved in G_2 cell cycle arrest. High and low concentrations of CPT produced qualitatively different changes in patterns of gene expression.

MATERIALS AND METHODS

Materials and Cell Culture

APH and CPT were purchased from Sigma Chemical Co.-Aldrich and dissolved in DMSO to concentrations of 3 and 10 mM, respectively. Cy3-dUTP, Cy5-dUTP, deoxynucleotide triphosphates, Oligo$(dT)_{12-18}$, and Oligo$(dA)_{40-60}$ were purchased from Amersham Pharmacia Biotech (Piscataway, NJ). Superscript II reverse transcriptase and hCOT-1 were purchased from Life Technologies, Inc. (Gaithersburg, MD). Seed cultures of human colon cancer cell line HCT116 were obtained from the Developmental Therapeutics Program, National Cancer Institute, and the cells were cultured in RPMI 1640 (Life Technologies, Inc.) containing 10% fetal bovine serum (BioAtlantic, GA) and 2 mM L-glutamine (Life Technologies, Inc.). The cells were grown to passage 19 and used in the experiments.

Cell Cycle Synchronization and CPT Treatment

HCT116 cells, cultured to near confluence, were trypsinized and plated at 3.6×10^6 cells/150-mm^2 dish (Becton Dickinson, Franklin Lakes, NJ). After

Received 6/1/01; accepted 1/14/02.

The costs of publication of this article were defrayed in part by the payment of page charges. This article must therefore be hereby marked *advertisement* in accordance with 18 U.S.C. Section 1734 solely to indicate this fact.

[1] Present address: Cellular Genomics Inc., 36 East Industrial Drive, Branford, CT 06405.

[2] To whom requests for reprints should be addressed, at Laboratory of Molecular Pharmacology, DBS, NCI, NIH, Building 37/5D-02, 37 Convent Drive MSC 4255, Bethesda, MD 20892-4255. Phone: (301) 496-5971; Fax: (301) 402-0752; E-mail: weinstein@dtpax2.ncifcrf.gov.

[3] The abbreviations used are: CPT, camptothecin; APH, aphidicolin; FACS, fluorescence *in situ* sorting; CIM, clustered image map; TRAF5, tumor necrosis factor receptor-associated factor 5; TGF, tumor growth factor.

a 24-h incubation, the cells were synchronized in medium containing 1 μM APH for 17 h or for the time indicated. CPT treatment was carried out as follows on synchronized cells after 17 h with APH. The APH-containing medium was removed, and the cells were washed twice with APH-free medium, and then cultured in drug-free medium for 2 h. Portions of the cells were then treated for 75 min with 0, 20, or 1000 nM CPT. In each case the medium contained 0.01% DMSO. The CPT/DMSO-containing medium was then removed, and the cells were washed twice with drug-free medium. Thereafter, cells were cultured in drug-free medium for the indicated time.

FACS Analysis of Cell Cycle Stage

Cells were trypsinized, and the resulting cell suspensions were centrifuged at 1000 rpm for 10 min. The cells were fixed by resuspending them in 0.5 ml of 70% ethanol for 30 min, centrifuging them at 1500 rpm for 10 min, and washing the pellets twice with ice-cold PBS to remove residual ethanol. The cell pellets were resuspended in 0.5 ml of PBS containing 50 μg/ml propidium iodide (Sigma Chemical Co.-Aldrich, St. Louis, MO) and 100 μg/ml RNase (Sigma-Aldrich), incubated at 37°C for 30 min, and then analyzed using a FACScan flow cytometer (Becton Dickinson).

cDNA Microarray Analysis of Gene Transcription

Total RNA was isolated from cells by the RNeasy Midi Kit (Qiagen, Valencia, CA) and concentrated to 5 μg/μl in diethyl pyrocarbonate-treated water (Research Genetics, Huntsville, AL). The RNA samples were aliquoted and stored at −70°C. cDNA microarray experiments were carried out using a protocol developed by the Laboratory of Cancer Genetics of the National Human Genome Research Institute,[4] with minor modifications. Cy3 and Cy5 labeling was done with 54 and 72 μg of total RNA, respectively. Seventy-five μM Cy3-dUTP or Cy5-dUTP was used in each labeling reaction. Cy3- and Cy5-labeled cDNA samples, one experimental and the other a reference sample, were mixed in equal amounts. The mixture was then hybridized with a pin-spotted cDNA microarray. The microarrays were spotted robotically at the National Cancer Institute Microarray Facility, Advanced Technology Center. Each microarray contained 2076 cDNA spots corresponding to known cancer-related genes. Some of the genes were printed on the microarray more than once to provide replicates for reproducibility analysis.[5] The hybridization data were acquired using the Avalanche Fluorescence Scanner (Molecular Dynamics, Sunnyvale, CA). Image analysis was carried out using a set of software tools developed by Y. Chen (15) at the Laboratory of Cancer Genetics, National Human Genome Research Institute.[6]

To remove the systematic bias caused by the chemical difference between Cy3 and Cy5, each microarray study was performed twice using "reciprocal labeling," *i.e.*, for the first microarray, the experimental sample was labeled with Cy3 and the reference sample was labeled with Cy5, whereas for the second microarray, the reference sample was labeled with Cy3 and the experimental sample was labeled with Cy5. Throughout the data analysis process, differential expression was represented by:

$$GMR_i = \sqrt{\left(\frac{E_{cy3_1}}{R_{cy5_1}}\right) \cdot \left(\frac{E_{cy5_2}}{R_{cy3_2}}\right)} \qquad \text{(A)}$$

where GMR_i denotes the geometric mean of ratios, *1* and *2* denote the two arrays used, *i* denotes the array pair, and *E* and *R* denote the experimental and reference samples, respectively.

Data Analysis

Data Preprocessing. Before any of the analyses, we removed the data from empty spots and reagent-control spots [poly(dA), Cot I, Cy3, and Cy5]. On each array, 2076 of the original 2208 spots remained, and 242 of those spots were in duplicate. We also removed data from spots identified as visibly flawed (<20 in all for the 36 arrays). We then normalized the ratio data by Gaussian-kernel fitting[7] and normalized the resulting values for each cell type so that the sum of the log-transformed values was the same for each cell sample. We next filtered the data to obtain genes whose expression differed by more than 1.7-fold in the reciprocal-averaged ratio (GMR_i). This threshold criterion was, to a degree, arbitrary. It was based, however, on quality control experiments in which we found that >99% of spots had reciprocal-averaged ratios between 1.7 and 1/1.7 when two identical samples were analyzed (Fig. 3). In addition, to further remove possible outliers (such as, *e.g.*, the three points in the *right panel* of Fig. 3), we selected only spots that met the 1.35-fold change criterion for both of the duplicate arrays. We further required that the data point meet these criteria for more than 1 design point in the set of 18. This procedure selected a total of 33 different genes, including 3 that were represented twice in the microarray.

Cluster Analysis and CIMs. Most statistical analyses were carried out using Matlab 5.3 (Mathworks Inc., Natick, MA). We clustered the genes using agglomerative hierarchical average-linkage based on the Euclidian distance metric. For each gene, the ratio value was based on the reciprocal average, as shown in Eq. A. The data are presented in the form of color-coded CIMs generated in Matlab. We introduced CIMs previously for compact visualization of "high dimensional" biological and pharmacological data (16–18), and they have since been used by others (19). In the CIMs here, only the genes were clustered (to bring similar expression patterns together); the experiments were left in natural order.[8]

RESULTS

Cell Cycle Synchronization and CPT Treatment

The protocol is summarized in Fig. 1. To obtain a relatively homogeneous cell population before CPT treatment, we synchronized HCT116 cells using APH. APH, an inhibitor of DNA polymerase α, blocks the cell cycle in S-phase. HCT116 cells have a doubling time of 16 h, and incubation of HCT116 cells with 1 μM APH for 17 h arrested most cells in S-phase. Cell cycling resumed immediately after removal of APH. After 17 h of exposure to APH and 2 h in APH-free medium, ~80% of the cells were still in S-phase. The cells were then treated with or without CPT for 75 min and finally incubated in CPT-free medium for the times indicated in Fig. 1.

Cell cycle progression after APH synchronization and CPT treatment was examined using FACS after different times of culture in drug-free medium. Subpopulations of cells containing 2N (G_1 phase) and 4N (G_2 phase) DNA were separated into two distinct peaks. A FACS study of dose dependence (over a range from 1 nM to 10 μM CPT) identified CPT concentrations that caused reversible and irreversible G_2 arrest (results not shown). Gene expression changes were measured after treatment with 0, 20, or 1000 nM CPT. As shown in Fig. 2, the cells not treated with CPT resumed cell cycle progression after removal of APH, and the time taken to complete the first cycle was close to the normal doubling time of HCT116 cells. The cells treated with 20 nM CPT slowed down slightly in S-phase and were significantly delayed in G_2-M. The apparent G_2-M phase of cells treated with 20 nM CPT was approximately twice as long as that of the control cells (0.01% DMSO). The cells treated with 1000 nM CPT showed significant S-phase delay (8–10 h), and G_2-M arrest was not reversed even after a 60-h incubation in drug-free medium (data not shown).

cDNA Microarray Analysis of Gene Expression

Data Acquired Using cDNA Microarrays. The microarray studies included two series of experiments. The first series examined changes in gene expression caused by CPT treatment. In these experiments, total RNA was isolated from cells harvested at the time points indicated in Fig. 1, and the reference sample was total RNA isolated from cells harvested at the end of the 17-h APH synchronization (2 h

[4] http://www.nhgri.nih.gov/DIR/LCG/15K/HTML/protocol.html.
[5] The gene list can be found at http://nciarray.nci.nih.gov/gi_acc_ug_title.shtml.
[6] http://www.nhgri.nih.gov/DIR/LCG/15K/HTML/.
[7] L. H. Smith *et al.*, New methods for analysis of two-color microarray data, manuscript in preparation.
[8] A versatile program for producing CIMs can be found at http://discover.nci.nih.gov.

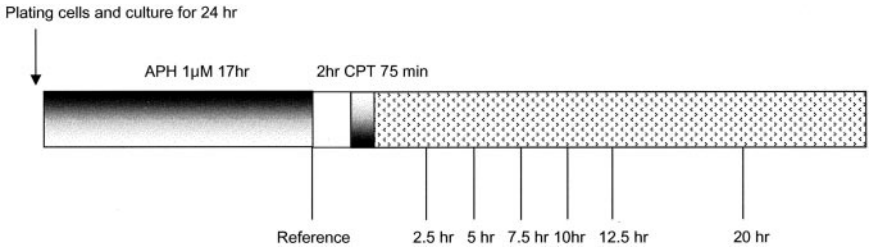

Fig. 1. Schematic of the experimental protocol.

before CPT treatment). This series generated 36 microarray data sets, *i.e.*, 18 reciprocally labeled pairs of arrays. Included were duplicate sets for cells collected 5 h after treatment with 1000 nM CPT.

The second series of experiments examined the effects of APH treatment on gene expression. In these experiments, total RNA isolated from APH-treated cells was compared with total RNA isolated from nontreated cells. The APH treatment was carried out for 6, 12, 17, and 24 h. This series of experiments produced 10 microarray data sets, *i.e.*, 5 reciprocally labeled pairs of arrays. Included were duplicate data sets for cells harvested after 17 h of treatment with APH. In addition, to evaluate random variation in the experimental procedure, we carried out 17-h APH synchronization three different times using the same conditions, and the three independent samples were compared with each other in pairwise fashion. After calibrating the signals from both the Cy3 and Cy5 channels and averaging the ratios of two reciprocally labeled duplicates, we found that >99% of the genes in the three control data sets showed ratio differences <1.7-fold (Fig. 3). Data reproducibility was also assured by the high correlation between duplicate gene pairs (represented by the same clone or different clones). As illustrated in Fig. 4, the duplicate clones clustered together.

CIM Analysis of Selected Genes in CPT-treated Samples. To identify changes in gene expression induced by drug treatment and to remove random noise (isolated spikes) in the data sets, we filtered the data to obtain genes whose expression differed at more than one experimental time point by >1.7-fold in either direction from the reference for the reciprocally averaged pair and by >1.35-fold for both of the arrays. A total of 33 genes met those criteria, and 3 of them were represented twice on the microarray chip. Thus, we selected a total of 36 cDNA spots. Expression data for the 36 spots from 18 CPT experiments were clustered based on the expression patterns and represented in the form of a CIM (Fig. 4). The gene definitions were based on human Unigene build #95.

Clustering the genes brings out patterns in the data by grouping together genes with similar expression profiles. Of the 33 genes that exhibited changes according to the criteria established, 27 clustered tightly within three groups (Fig. 4*A*). Group I genes were up-regulated in the control and low-dose CPT-treated cells, but the up-regulation took place at a later time in cells treated with low-dose CPT. The difference in timing of up-regulation closely matched the difference in the timing of mitosis. Those genes were not up-regulated after high-dose CPT treatment. Group II genes were down-regulated during the period of time when low-dose CPT-treated cells were recovering from G_2 delay. In the case of high-dose CPT treatment, some of these genes showed an abortive down-regulation shortly after drug removal. Group III genes were up-regulated in the cells treated with high-dose CPT during S-phase delay and/or G_2 arrest, but these genes did not change in the cells treated with low-dose CPT. Time-dependent expression changes for the 36 spots are shown in a line graph in Fig. 4*B*.

The changes in expression identified by cDNA microarray were largely consistent with the results obtained using Northern blot analysis (Table 1). In summary, Northern blot analyses were run for five of the genes, each over eight experimental conditions. IMP dehydrogenase 1, which showed no significant difference in ratio from sample to sample in the microarray analysis, was used as a normalization reference. The overall Pearson correlation coefficients (r) relating microarray and Northern expression levels for the eight conditions were as follows: for *p21*, $r = 0.88$; for *14-3-3σ*, $r = 0.92$; for *cyclin B1*, $r = 0.79$; for *aurora/IPL1*, $r = 0.91$; for *p16-INK4a*, $r = 0.78$.

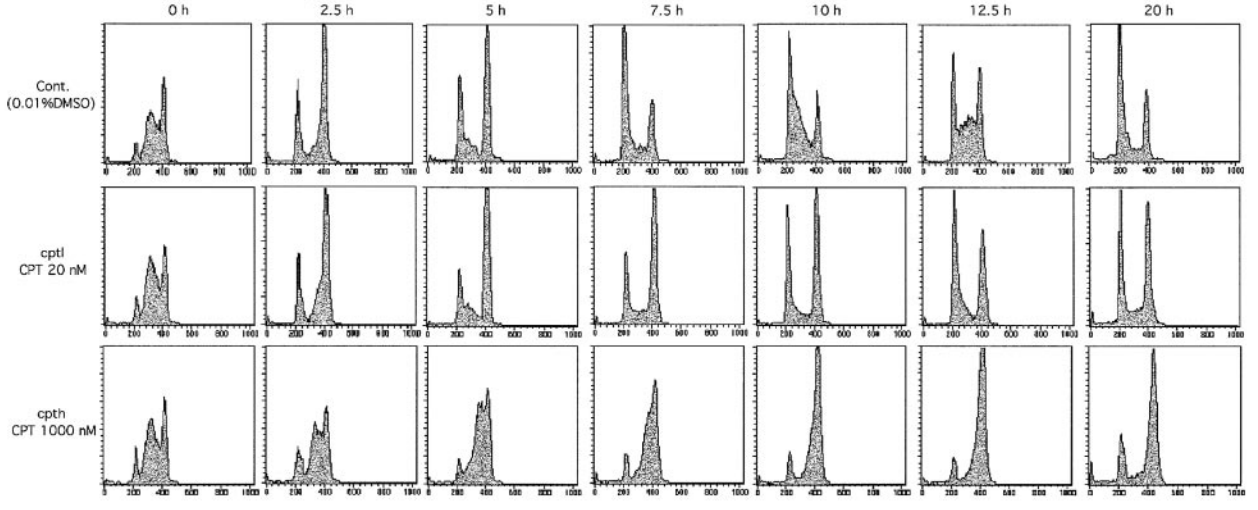

Fig. 2. *A*, FACS analysis of cell cycle progression at indicated time points. Fluorescence intensity representing the cellular DNA content is shown on the *X axis*, and cell count is shown on the *Y axis*. A total of 10,000 events were collected in FACS analysis. The *left-hand peak* in each *panel* represents G_1 cells, the *right-hand peak* represents G_2 cells, and the points *between* represent S-phase cells. *Cont.*, control.

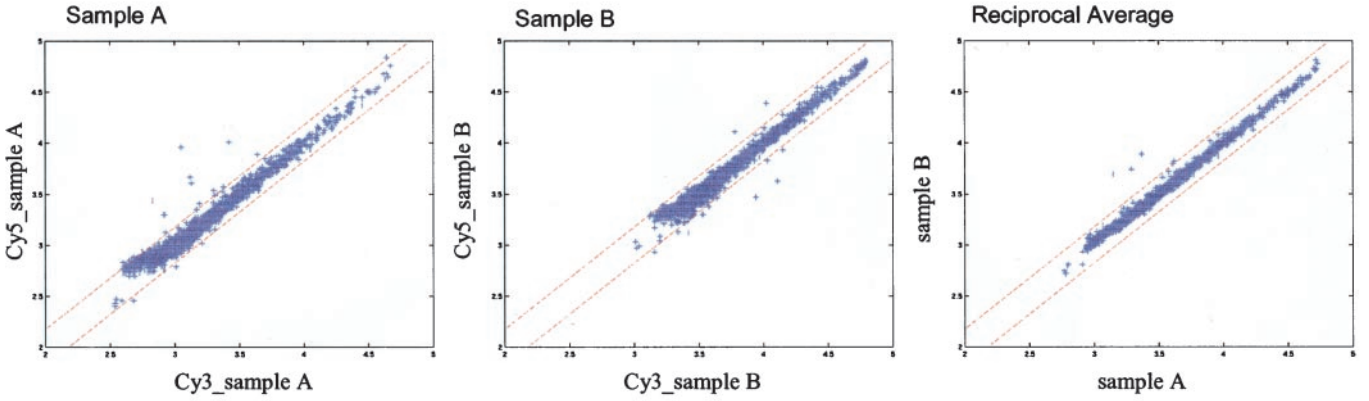

Fig. 3. System noise determined through comparison of cells receiving identical APH treatment in different experiments. Total RNA was isolated from cells treated with 1 μM APH for 17 h. *X* and *Y axes* for *Samples A* and *B* represent $\log_{10}$-transformed intensity values. *X* and *Y axes* in the *Reciprocal Average panel* represent $\log_{10}$-transformed average intensity values for the two slides (calculated as described in the text). *Dashed lines* indicate 1.5-fold differences between samples.

The overall average of the correlation coefficients for the five genes was, therefore, $r = 0.86$

Expression of the 33 Genes in APH-treated Samples. To assess the effect of APH treatment itself on gene expression, we examined data for the 36 spots from the five APH time points. The 36 spots were ordered in Fig. 4 according to the cluster order generated from the CPT experimental data. The results are shown in the five columns at the *right side* of the CIM in Fig. 4. The group I genes were down-regulated in most of the APH-treated cells, whereas some of the group III genes were up-regulated in the cells treated with APH for 17 and 24 h. Group II genes did not show any consistent changes.

DISCUSSION

The basic mechanism of action for CPT has been well studied and characterized (1, 2). CPT generates replication-mediated double-strand DNA breaks, which in turn induce reversible or permanent cell cycle arrest in G_2-M. In this study, we used cDNA microarrays to investigate the molecular consequences of CPT's activity at the transcriptional level. Among other observations, we found that reversible cell cycle arrest in G_2-M after low-dose CPT treatment was associated with delayed up-regulation of mitosis-related genes, which are normally up-regulated during G_2. In contrast, treatment with high-dose CPT elevated expression of some p53-responsive genes.

To study dose- and time-dependent effects of CPT treatment on cell cycle progress and gene expression, we carried out the experiments using APH-synchronized cells treated with 1000, 20, or 0 nM CPT (all in 0.01% DMSO). The time dependence of treatment effects was revealed by comparing each sample with an internal second-color control harvested after synchronization with APH but without any other treatment. This direct comparison of all CPT- and sham-treated samples with a single internal control permitted us to map out the time course of expression levels after treatment.

Because the cytotoxicity of CPT is cell-cycle specific and because CPT treatment directly affects cell cycle progression, we reasoned that we could optimize our chance of seeing down-regulations and modest up-regulations of genes if we synchronized the cells and then treated them at the appropriate point in the cell cycle. Among the possible methods (none of them perfect) for synchronizing cells, we selected the commonly used technique based on incubation with APH, an inhibitor of DNA polymerases. However, APH itself can induce gene expression changes. It can activate p53 and up-regulate p21/WAF1 expression (20). Mitosis may also be perturbed immediately after treatment with high-dose APH (21). To minimize (although not completely eliminate) such confounding influences, we used a minimum concentration of APH for synchronization. In this study, we did not observe perturbation of mitosis after removal of APH (Fig. 2), and a colony formation assay did not indicate significant toxicity (data not shown). To monitor gene expression changes caused by APH treatment, we compared gene expression in cells incubated with and without APH. Stress-related responses, including moderate elevation of p21/WAF1 transcript, were observed after prolonged APH treatment (Fig. 4*A*), but they had little effect on cell cycle progression after removal of APH. Because the internal control for the APH experiments was an unsynchronized cell sample and that for the CPT-treatment experiments was an APH-treated sample, the appearance of up-regulated gene expression after CPT treatment indicated an additional up-regulation above the already increased expression caused by APH. For example, p53-responsive genes were up-regulated after APH treatment. Subsequent treatment with high-dose CPT induced additional up-regulation, whereas treatment with low-dose CPT or no CPT largely maintained the already elevated transcription levels.

On the basis of cluster analysis (Fig. 4*A*), the 33 changing genes fell into three predominant groups based on their patterns of gene expression:

Group I Genes. Group I genes tended to be maximally up-regulated during the time that cells were in transit through G_2-M. Their increased expression correlated well with the period of time during which most of the APH-treated control cells or the low-dose CPT-treated cells were beginning to exit from mitosis. Among six genes in this group, *cyclin B1*, *aurora/STK15*, *Nek2*, and *hRad6* are directly involved in mitotic regulation. Through formation of a complex with CDK1 ($p34^{cdc2}$), cyclin B1 promotes entry into mitosis, and its expression is tightly regulated in the cell cycle. Its expression is low in G_1 but up-regulated throughout the S and G_2 phases (22). Cyclin B1 associates with centrosomes at about the time of transition of the centrosome's microtubule organizing center from an interphase to a mitotic pattern (Ref. 23 and references cited therein). STK15, a member of the aurora/IPL1 kinase family, is a short-lived protein associated with the mitotic spindle and centrosome. It is required for cell cycle progression and genome stability (24, 25). The *STK15* gene is amplified and overexpressed in multiple human tumor cell types and can induce excessive centrosome duplication. Nek2 is another protein kinase whose expression is up-regulated during the S and G_2 phases. Nek2 is a core component of the centrosome. It is probably required for separation of centrosomes and for the G_2-to-M transition (26–28). *hRad6* codes a ubiquitin-conjugating enzyme critical for

A

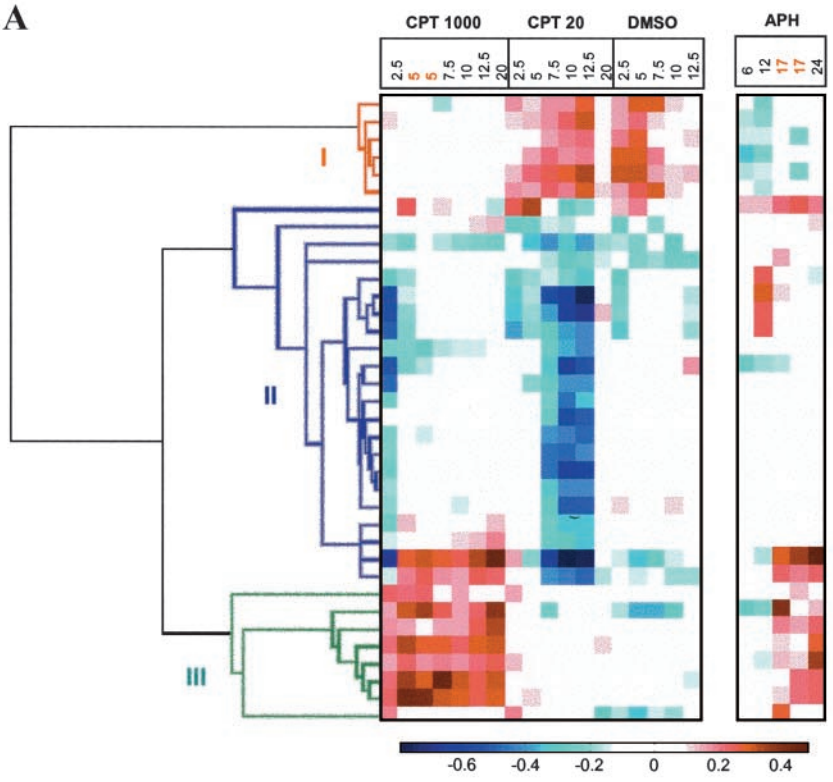

Clone ID	Order	Gene definition
563130	1.	Cyclin B1
1422081	2.	Nek2 protein kinase
937230	3.	TRAF5=TNF receptor associate factor 5
898138	4.	Ubiquitin-conjugating enzyme E2B (RAD6 homolog)
209066	5.	STK15-aurora/IPL1-related kinase
550316	6.	p16-INK4a=Cyclin-dependent kinase 4 inhibitor
136590	7.	Tissue factor=transmembrane glycoprotein cofactor *
248828	8.	Id-3=helix-loop-helix transcription factor *
345603	9.	Insulin induced protein 1= INSIG1 *
246619	10.	Cytochrome p450 subfamily IIC *
265267	11.	HSP70
50615	12.	HSP70-HOM=Heat shock 70 KD protein 1
50615	13.	HSP70-HOM=Heat shock 70 KD protein 1
265267	14.	HSP70
627173	15.	Protein phosphatase 3 (calcineurin A alpha)
824602	16.	Interferon-gamma induced protein (IFI 16) gene
460538	17.	Glutathione reductase
327094	18.	Similar to calcium/calmodulin-dependent protein kinase
223122	19.	Protein phosphatase with EF-hands-2 long form (PPEF-2)
897619	20.	XE7=B-lymphocyte surface protein
357421	21.	CaM kinase II isoform
531487	22.	GS2 protein (DXS1283E)
161373	23.	PMS6 (yeast mismatch repair gene PMS1 homologue)
362926	24.	PKA-C-BETA=cAMP-dependent protein kinase
1175007	25.	Decoy receptor 2
1117041	26.	MHC class 1 protein HLA-G
470149	27.	p21=cyclin kinase inhibitor *
346610	28.	14-3-3 sigma*
149994	29.	B12 protein
549383	30.	TGF-beta superfamily protein
742132	31.	Interferon-induced 17 KD protein
243882	32.	protein phosphatase Wip1
115295	33.	Damage-specific DNA binding protein 2 (48 kD)
299745	34.	CD95=Fas
299745	35.	CD95=Fas
813552	36.	CD47 antigen

B

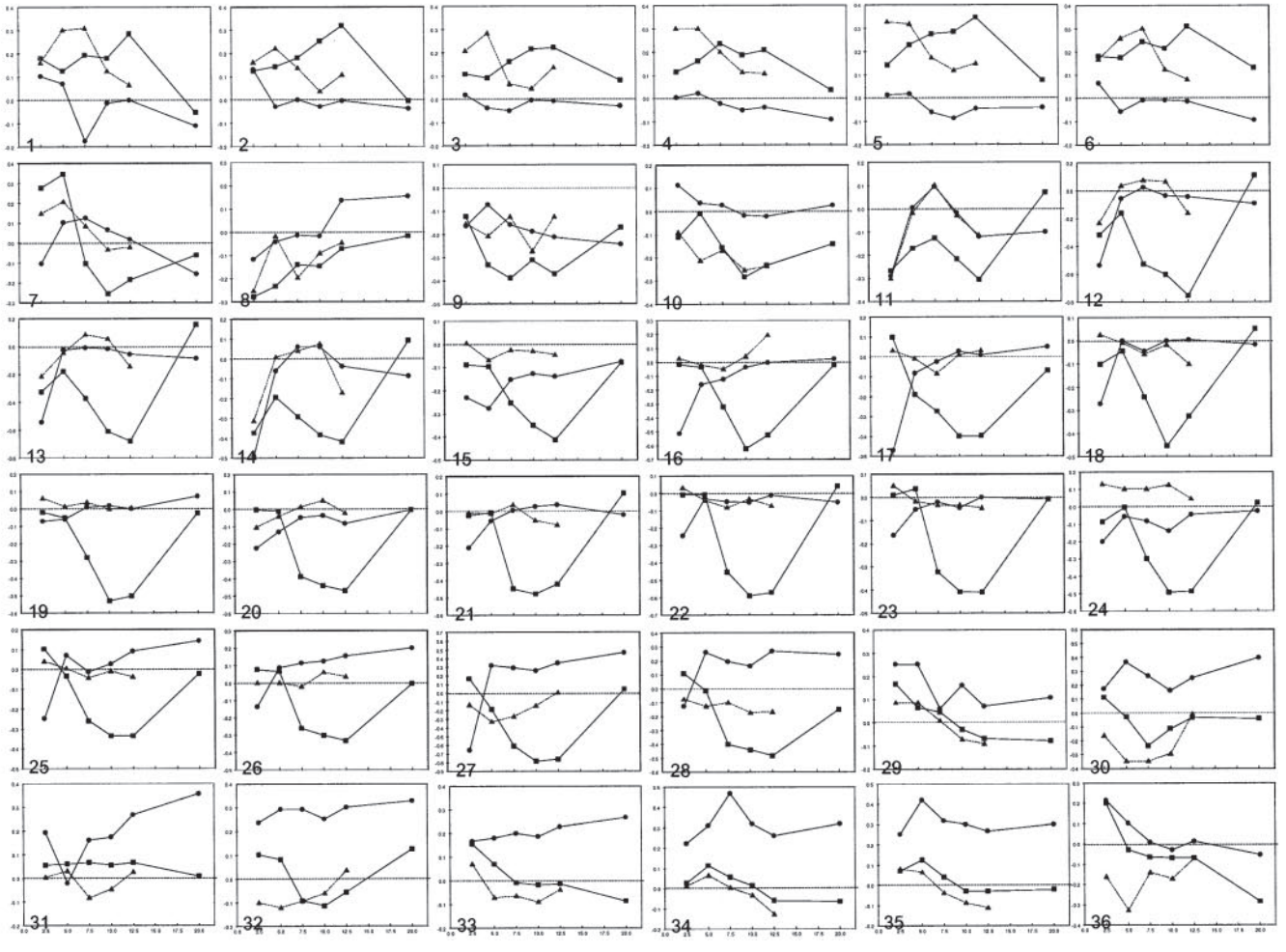

Table 1 *Consistency between results obtained using cDNA microarrays and Northern analysis*[a]

	p21		14-3-3 σ		Cyclin B1		aurora/IPL1		p16-INK4a	
	Microarray	Northern	Microarray	Northern	Microarray	Northern	Microarray	Northern	Microarray	Northern
Reference	1.0	1.0	1.0	1.0	1.0	1.0	1.0	1.0	1.0	1.0
cpth[a] 5	2.1	2.2	1.8	1.9	1.2	1.1	1.0	0.5	0.9	0.7
cpth 12.5	2.2	2.3	1.9	2.4	1.0	1.2	0.9	0.6	1.0	0.7
cptl 5	0.7	0.7	1.0	1.0	1.3	2.0	1.7	1.3	1.5	1.0
cptl 7.5	0.2	0.8	0.4	0.7	1.6	3.2	1.9	2.5	1.8	2.0
cptl 12.5	0.2	1.2	0.3	0.6	1.9	4.1	2.2	2.6	2.0	2.6
cont 2.5	0.7	0.7	0.8	0.5	1.4	1.8	2.1	1.9	1.5	1.3
cont 5	0.5	0.4	0.7	0.5	2.0	4.0	2.1	3.1	1.8	2.5
cont 7.5	0.5	0.4	0.8	0.5	2.0	2.1	1.5	1.3	2.0	1.3

[a] cpth, treatment with 1000 nM CPT; cptl, treatment with 20 nM CPT; cont, treatment with 0.01% DMSO.

degradation of proteins that maintain the G_2 or M states of the cell (29). When analyzing a CIM of the entire 1694-gene data set (results not shown), we identified a tight cluster branch that contained all of the group I genes as well as other genes showing expression patterns similar to those of group I but not meeting the criteria used to select the set of 33 genes. That branch is shown in Fig. 5. Most of the additional genes are mitosis related. Among them, ckshs2 and CENP-F kinetochore protein have been shown to have regulated expression patterns similar to that of cyclin B1 (30).

The mitosis-related function and changes in expression level during cell cycle suggest that up-regulation of this group of genes is a part of the cell cycle-regulatory mechanism in G_2-S. It is well established that DNA damage inhibits cyclin B1 expression and relocalizes cyclin B1 protein to the cytoplasm (29, 31, 32). The inhibition of cyclin B1 expression may be attributable to an increase in active p53 protein (33, 34). As noted above, in addition to cyclin B1, we found that CPT treatment delayed or inhibited the up-regulation of several other mitosis-related genes. This inhibition occurred before completion of DNA replication when cells were still in S or S-like phase. The disruption of transcriptional regulation suggests that cells arrested in G_2-like phase after DNA damage are different from normal G_2 cells. Although DNA replication was apparently completed, those cells may have been missing necessary mitotic machinery and therefore not have been ready to proceed to mitosis. This lack of complete mitotic machinery may be involved in G_2 arrest and mitotic catastrophe. The latter occurs in some types of cells after G_2 arrest after DNA damage (14, 35, 36). At this time, we do not know the upstream event that caused disruption of transcriptional regulation, and we do not know how this event relates to the G_2 checkpoint. However, it seems unlikely that the disruption of transcriptional regulation in cell cycle is directly attributable to p53 activation because the inhibition of mitotic gene expression could occur without further activation of genes in the p53 pathway (see below).

The implication of TRAF5 and p16-INK4a in group I is not clear at this point. TRAF5 is an adapter protein that links signaling from tumor necrosis factor receptor to nuclear factor-κB and to the apoptosis-regulating kinase ASK1 (37, 38). Via both mechanisms, TRAF5 tends to protect cells from apoptosis. p16-INK4a tends to block entry into S-phase by binding to cdk4/6, thereby preventing the activation of cdk4/6 by cyclin D. In all of our experiments, p16-INK4a exhibited expression patterns very similar to those of cyclin B1. This behavior is consistent with reports of p16 accumulation during G_2 delay of UV-treated HeLa cells (Ref. 39 and references cited therein).

Group II Genes. These genes were down-regulated during the period of G_2 delay in the cells treated with low-dose CPT. This down-regulation seemed not to be associated with G_2 *per se* because it was not seen in control cells as they passed through G_2, nor in the early period of G_2 delay in the cells treated with low-dose CPT. It was only during the extension of G_2 that the down-regulation occurred. This finding suggests that the down-regulation of group II genes is intimately related to a checkpoint that reversibly delays the transition from G_2 to mitosis. The absence of down-regulation in the high-dose CPT experiment suggests that most of the cells that were in S-phase during CPT treatment never reached a normal G_2 state. Some genes in this experiment showed an immediate transient down-regulation, perhaps reflecting the subpopulation of cells that were already at or near G_2 at the time of CPT treatment (see Fig. 2). The group II genes are heterogeneous in function, and they have not been associated previously with DNA damage response or normal cell cycle regulation. Some of them are associated with calcium-dependent pathways, cellular metabolism, and signal transduction pathways.

Group III Genes. Group III genes are characterized by increased expression after high-dose, but not low-dose, CPT treatment. These genes are inducible by DNA damage and are associated with cell cycle arrest and apoptosis. Five of the eight genes in the group are known to block cell cycle progression and to be activated by p53 in response to DNA damage: (*a*) the cyclin-dependent kinase inhibitor *p21* (35, 40); (*b*) the chaperone *14-3-3*σ (14, 41); (*c*) the type IIC protein phosphatase *Wip1* (42, 43); (*d*) the apoptosis-inducer *CD95/Fas* (44); and (*e*) the damage-specific DNA-binding protein subunit *DDB2* gene (45). HCT116 is p53 wild type and exhibits p53 function (13). It is possible that the up-regulation of p53-responsive genes in HCT116 after high-dose CPT treatment was attributable to activation of p53. Although we do not have direct data on p53 protein in these experiments, this pattern of up-regulation of five p53-responsive genes in these p53 wild-type cells strongly suggests that p53 protein activity was up-regulated after high-dose CPT treatment. These observations are consistent with present understanding of the transcriptional role of p53 in cellular responses to DNA damage.

In contrast to the observation with high-dose CPT, group III genes showed no up-regulation after low-dose CPT treatment, suggesting that p53-dependent cell death- and cell cycle-related genes were not

Fig. 4. *A*, CIM for 33 genes that changed expression sufficiently as a consequence of CPT treatment to meet criteria described in the text. Each *column* represents an experimental configuration. *CPT 1000*, treatment with 1000 nM CPT in 0.01% DMSO; *CPT 20*, treatment with 20 nM CPT in 0.01% DMSO; *DMSO*, control with 0.01% DMSO; *APH*, treatment with 1 μM APH in 0.01% DMSO. The *numbers* at the *top* of the figure indicate the time in hours after removal of CPT (or control DMSO) or the duration in hours of treatment with APH. *Red numbers* indicate replicate experiments performed at different times. *Red boxes* indicate high expression, *blue boxes* indicate low expression, and *white boxes* indicate intermediate expression. *, genes that show mixed or ill-defined patterns. The three pairs of duplicate genes are indicated by *brackets* on the *right*. The scale reflects $\log_{10}$-transformed ratio value. *B*, time courses of expression levels for the 33 genes (plus 3 duplicates). Genes are numbered in the order in which they appear in *A*. Time (h) on the *X axis* represents the time after removal of CPT (or DMSO). The *horizontal line* in each panel indicates no change in gene expression. ▲, treatment with 0.01% DMSO; ■, treatment with 20 nM CPT in 0.01% DMSO; ●, treatment with 1000 nM CPT in 0.01% DMSO.

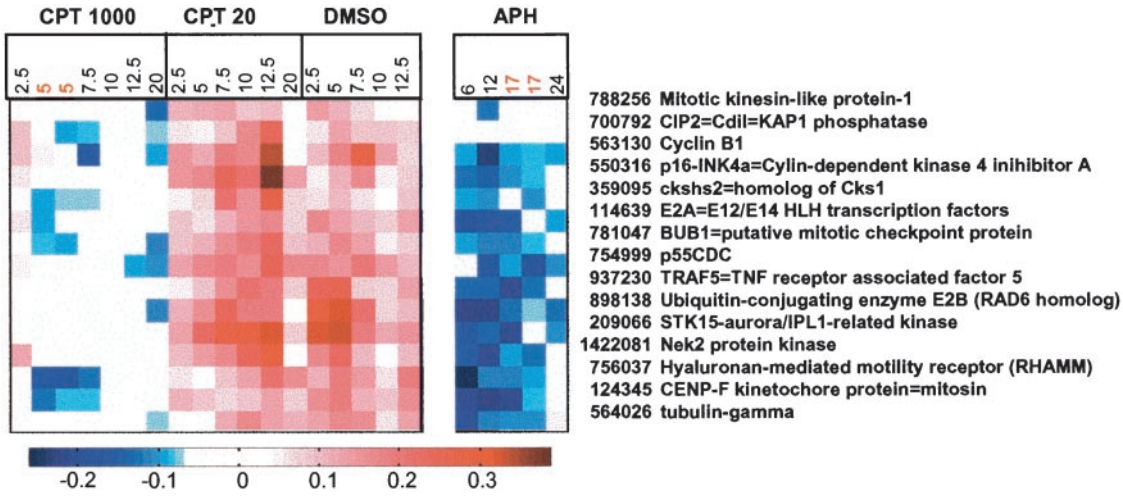

Fig. 5. Branch of the cluster analysis of the entire data set containing all group I genes as well as other genes showing expression patterns similar to those of group I but not picked up by the criteria used to select the set of 33 genes. Experimental conditions listed at the *top* are denoted as in the legend to Fig. 4. *Red* indicates high expression, *blue* indicates low expression, and *white* indicates intermediate expression.

significantly up-regulated under conditions of reversible cell cycle arrest. Two of the p53-responsive genes (*p21* and *14-3-3σ*) were in fact down-regulated, perhaps reflecting recovery from the up-regulation induced by exposure to APH. This behavior suggests a remarkable distinction between the reversible G_2 delay seen in these experiments after low-dose CPT treatment and the more permanent G_2 arrest that followed extensive DNA damage after high-dose CPT.

In addition to p53-responsive genes, group III also included the genes for TGF-β superfamily protein and IFN-induced 17-kDa protein. The TGF-β superfamily protein is involved in signal transduction events that regulate cell growth and differentiation (46). It has been reported to be up-regulated in cells treated with the DNA topoisomerase II inhibitor VP-16 (47). The highly correlated expression pattern seen here indicates a possible relationship of TGF-β superfamily protein to DNA damage and p53 activity, although such associations have not previously been reported.

In conclusion, we find it striking that 27 of the 33 genes selected objectively from the overall set of 1694 represented on the microarrays fell coherently into three tightly clustered patterns of behavior. These patterns appear to define signatures for the initial molecular consequences of CPT treatment. Even more unexpected, changes in gene expression during the first cell cycle after treatment revealed patterns after a relatively nontoxic dose of CPT that were qualitatively different from those after a highly toxic dose, although there was no gross cell death during the course of the experiments in either case. We were not surprised to see that the high dose precipitated broad changes not seen at the low dose, but we were surprised to find that the reverse was also true, that the low dose led to changes not seen at the high dose. On the basis of these observations, we propose that there is a fundamental difference between the gene expression changes associated with reversible G_2 delay that follows mild DNA damage and permanent G_2 arrest that follows more extensive DNA damage. The fate of cells after DNA damage is probably determined by coordination and balancing of multiple parallel processes at both the transcription and protein levels. Directed experimental investigations will be required to test the hypotheses generated by these microarray experiments. In particular, it will be instructive to follow up the suggestion of these experiments that the differences involve patterns of regulation in the pathways of *p53* and other stress-response genes, as well as in the mitotic machinery, especially with regard to centromere formation and function.

REFERENCES

1. Strumberg, D., Pilon, A. A., Smith, M., Hickey, R., Malkas, L., and Pommier, Y. Conversion of topoisomerase I cleavage complexes on the leading strand of ribosomal DNA into 5′-phosphorylated DNA double-strand breaks by replication runoff. Mol. Cell. Biol., *20:* 3977–3987, 2000.
2. Pommier, Y., Pourquier, P., Fan, Y., and Strumberg, D. Mechanism of action of eukaryotic DNA topoisomerase I and drugs targeted to the enzyme. Biochim. Biophys. Acta., *1400:* 83–105, 1998.
3. Darzynkiewicz, Z., Bruno, S., Del Bino, G., and Traganos, F. The cell cycle effects of camptothecin. Ann. NY Acad. Sci., *803:* 93–100, 1996.
4. Murren, J. R., Beidler, D. R., and Cheng, Y. C. Camptothecin resistance related to drug-induced down-regulation of topoisomerase I and to steps occurring after the formation of protein-linked DNA breaks. Ann. NY Acad. Sci., *803:* 74–92, 1996.
5. Goldwasser, F., Bae, I., Valenti, M., Torres, K., and Pommier, Y. Topoisomerase I-related parameters and camptothecin activity in the colon carcinoma cell lines from the National Cancer Institute anticancer screen. Cancer Res., *55:* 2116–2121, 1995.
6. Wuerzberger, S. M., Pink, J. J., Planchon, S. M., Byers, K. L., Bornmann, W. G., and Boothman, D. A. Induction of apoptosis in MCF-7:WS8 breast cancer cells by β-lapachone. Cancer Res., *58:* 1876–1885, 1998.
7. Liu, W., and Zhang, R. Upregulation of p21WAF1/CIP1 in human breast cancer cell lines MCF-7 and MDA-MB-468 undergoing apoptosis induced by natural product anticancer drugs 10-hydroxycamptothecin and camptothecin through p53-dependent and independent pathways. Int. J. Oncol., *12:* 793–804, 1998.
8. Ross, D. T., Scherf, U., Eisen, M. B., Perou, C. M., Rees, C., Spellman, P., Iyer, V., Jeffrey, S. S., Van de Rijn, M., Waltham, M., Pergamenschikov, A., Lee, J. C., Lashkari, D., Shalon, D., Myers, T. G., Weinstein, J. N., Botstein, D., and Brown, P. O. Systematic variation in gene expression patterns in human cancer cell lines. Nat. Genet., *24:* 227–235, 2000.
9. Scherf, U., Ross, D. T., Waltham, M., Smith, L. H., Lee, J. K., Tanabe, L., Kohn, K. W., Reinhold, W. C., Myers, T. G., Andrews, D. T., Scudiero, D. A., Eisen, M. B., Sausville, E. A., Pommier, Y., Botstein, D., Brown, P. O., and Weinstein, J. N. A gene expression database for the molecular pharmacology of cancer. Nat. Genet., *24:* 236–244, 2000.
10. Schena, M., Shalon, D., Davis, R. W., and Brown, P. O. Quantitative monitoring of gene expression patterns with a complementary DNA microarray. Science (Wash. DC)., *270:* 467–470, 1995.
11. Schena, M., Shalon, D., Heller, R., Chai, A., Brown, P. O., and Davis, R. W. Parallel human genome analysis: microarray-based expression monitoring of 1000 genes. Proc. Natl. Acad. Sci. USA, *93:* 10614–10619, 1996.
12. DeRisi, J., Penland, L., Brown, P. O., Bittner, M. L., Meltzer, P. S., Ray, M., Chen, Y., Su, Y. A., and Trent, J. M. Use of a cDNA microarray to analyse gene expression patterns in human cancer. Nat. Genet., *14:* 457–460, 1996.
13. O'Connor, P. M., Jackman, J., Bae, I., Myers, T. G., Fan, S., Mutoh, M., Scudiero, D. A., Monks, A., Sausville, E. A., Weinstein, J. N., Friend, S., Fornace, A. J., Jr., and Kohn, K. W. Characterization of the p53 tumor suppressor pathway in cell lines of the National Cancer Institute anticancer drug screen and correlations with the growth-inhibitory potency of 123 anticancer agents. Cancer Res., *57:* 4285–4300, 1997.
14. Chan, T. A., Hermeking, H., Lengauer, C., Kinzler, K. W., and Vogelstein, B. 14-3-3σ is required to prevent mitotic catastrophe after DNA damage. Nature (Lond.), *401:* 616–620, 1999.
15. Chen, Y., Dougherty, E. R., and Bittner, M. L. Ratio-based decisions and quantitative analysis of cDNA microarray images. Biomed. Optics, *2:* 364–374, 1997.
16. Weinstein, J. N., Myers, T., Buolamwini, J., Raghavan, K., van Osdol, W., Licht, J., Viswanadhan, V. N., Kohn, K. W., Rubinstein, L. V., Koutsoukos, A. D., *et al.*

Predictive statistics and artificial intelligence in the U. S. National Cancer Institute's Drug Discovery Program for Cancer and AIDS. Stem Cells, *12:* 13–22, 1994.
17. Weinstein, J. N., Myers, T. G., O'Connor, P. M., Friend, S. H., Fornace, A. J., Jr., Kohn, K. W., Fojo, T., Bates, S. E., Rubinstein, L. V., Anderson, N. L., Buolamwini, J. K., van Osdol, W. W., Monks, A. P., Scudiero, D. A., Sausville, E. A., Zaharevitz, D. W., Bunow, B., Viswanadhan, V. N., Johnson, G. S., Wittes, R. E., and Paull, K. D. An information-intensive approach to the molecular pharmacology of cancer. Science (Wash. DC), *275:* 343–349, 1997.
18. Myers, T. G., Anderson, N. L., Waltham, M., Li, G., Buolamwini, J. K., Scudiero, D. A., Paull, K. D., Sausville, E. A., and Weinstein, J. N. A protein expression database for the molecular pharmacology of cancer. Electrophoresis, *18:* 647–653, 1997.
19. Eisen, M. B., Spellman, P. T., Brown, P. O., and Botstein, D. Cluster analysis and display of genome-wide expression patterns. Proc. Natl. Acad. Sci. USA, *95:* 14863–14868, 1998.
20. Ji, C., Marnett, L. J., and Pietenpol, J. A. Cell cycle re-entry following chemically-induced cell cycle synchronization leads to elevated p53 and p21 protein levels. Oncogene, *15:* 2749–2753, 1997.
21. Kung, A. L., Zetterberg, A., Sherwood, S. W., and Schimke, R. T. Cytotoxic effects of cell cycle phase specific agents: result of cell cycle perturbation. Cancer Res., *50:* 7307–7317, 1990.
22. Pines, J., and Hunter, T. Isolation of a human cyclin cDNA: evidence for cyclin mRNA and protein regulation in the cell cycle and for interaction with p34cdc2. Cell, *58:* 833–846, 1989.
23. De Souza, C. P., Ellem, K. A., and Gabrielli, B. G. Centrosomal and cytoplasmic Cdc2/cyclin B1 activation precedes nuclear mitotic events. Exp. Cell Res., *257:* 11–21, 2000.
24. Honda, K., Mihara, H., Kato, Y., Yamaguchi, A., Tanaka, H., Yasuda, H., Furukawa, K., and Urano, T. Degradation of human Aurora2 protein kinase by the anaphase-promoting complex-ubiquitin-proteasome pathway. Oncogene, *19:* 2812–2819, 2000.
25. Zhou, H., Kuang, J., Zhong, L., Kuo, W. L., Gray, J. W., Sahin, A., Brinkley, B. R., and Sen, S. Tumour amplified kinase STK15/BTAK induces centrosome amplification, aneuploidy and transformation. Nat. Genet., *20:* 189–193, 1998.
26. Fry, A. M., Arnaud, L., and Nigg, E. A. Activity of the human centrosomal kinase, Nek2, depends on an unusual leucine zipper dimerization motif. J. Biol. Chem., *274:* 16304–16310, 1999.
27. Fry, A. M., Descombes, P., Twomey, C., Bacchieri, R., and Nigg, E. A. The NIMA-related kinase X-Nek2B is required for efficient assembly of the zygotic centrosome in xenopus laevis. J. Cell Sci., *113:* 1973–1984, 2000.
28. Uto, K., and Sagata, N. Nek2B, a novel maternal form of Nek2 kinase, is essential for the assembly or maintenance of centrosomes in early *Xenopus* embryos. EMBO J., *19:* 1816–1826, 2000.
29. Jin, P., Hardy, S., and Morgan, D. O. Nuclear localization of cyclin B1 controls mitotic entry after DNA damage. J. Cell Biol., *141:* 875–885, 1998.
30. Iyer, V. R., Eisen, M. B., Ross, D. T., Schuler, G., Moore, T., Lee, J. C. F., Trent, J. M., Staudt, L. M., Hudson, J., Jr., Boguski, M. S., Lashkari, D., Shalon, D., Botstein, D., and Brown, P. O. The transcriptional program in the response of human fibroblasts to serum. Science (Wash. DC), *283:* 83–87, 1999.
31. Tsao, Y. P., D'Arpa, P., and Liu, L. F. The involvement of active DNA synthesis in camptothecin-induced G_2 arrest: altered regulation of p34cdc2/cyclin B. Cancer Res., *52:* 1823–1829, 1992.
32. Toyoshima, F., Moriguchi, T., Wada, A., Fukuda, M., and Nishida, E. Nuclear export of cyclin B1 and its possible role in the DNA damage- induced G_2 checkpoint. EMBO J., *17:* 2728–2735, 1998.
33. Innocente, S. A., Abrahamson, J. L. A., Cogswell, J. P., and Lee, J. M. p53 regulates a G_2 checkpoint through cyclin B1. Proc. Natl. Acad. Sci. USA, *96:* 2147–2152, 1999.
34. Badie, C., Itzhaki, J. E., Sullivan, M. J., Carpenter, A. J., and Porter, A. C. Repression of CDK1 and other genes with CDE and CHR promoter elements during DNA damage-induced G(2)/M arrest in human cells. Mol. Cell. Biol., *20:* 2358–2366, 2000.
35. Bunz, F., Dutriaux, A., Lengauer, C., Waldman, T., Zhou, S., Brown, J. P., Sedivy, J. M., Kinzler, K. W., and Vogelstein, B. Requirement for p53 and p21 to sustain G_2 arrest after DNA damage. Science (Wash. DC), *282:* 1497–1501, 1998.
36. Pines, J. Cell cycle. Checkpoint on the nuclear frontier. Nature (Lond.), *397:* 104–105, 1999.
37. Hoeflich, K. P., Yeh, W. C., Yao, Z., Mak, T. W., and Woodgett, J. R. Mediation of TNF receptor-associated factor effector functions by apoptosis signal-regulating kinase-1 (ASK1). Oncogene, *18:* 5814–5820, 1999.
38. Inoue, J., Ishida, T., Tsukamoto, N., Kobayashi, N., Naito, A., Azuma, S., and Yamamoto, T. Tumor necrosis factor receptor-associated factor (TRAF) family: adapter proteins that mediate cytokine signaling. Exp. Cell Res., *254:* 14–24, 2000.
39. Wang, X. Q., Gabrielli, B. G., Milligan, A., Dickinson, J. L., Antalis, T. M., and Ellem, K. A. Accumulation of p16CDKN2A in response to ultraviolet irradiation correlates with late S-G(2)-phase cell cycle delay. Cancer Res., *56:* 2510–2514, 1996.
40. el-Deiry, W. S., Tokino, T., Velculescu, V. E., Levy, D. B., Parsons, R., Trent, J. M., Lin, D., Mercer, W. E., Kinzler, K. W., and Vogelstein, B. WAF1, a potential mediator of p53 tumor suppression. Cell, *75:* 817–825, 1993.
41. Hermeking, H., Lengauer, C., Polyak, K., He, T. C., Zhang, L., Thiagalingam, S., Kinzler, K. W., and Vogelstein, B. 14-3-3σ is a p53-regulated inhibitor of G2/M progression. Mol. Cell, *1:* 3–11, 1997.
42. Fiscella, M., Zhang, H., Fan, S., Sakaguchi, K., Shen, S., Mercer, W. E., Vande Woude, G. F., O'Connor, P. M., and Appella, E. Wip1, a novel human protein phosphatase that is induced in response to ionizing radiation in a p53-dependent manner. Proc. Natl. Acad. Sci. USA, *94:* 6048–6053, 1997.
43. Choi, J., Appella, E., and Donehower, L. A. The structure and expression of the murine wildtype p53-induced phosphatase 1 (Wip1) gene. Genomics, *64:* 298–306, 2000.
44. Muller, M., Wilder, S., Bannasch, D., Israeli, D., Lehlbach, K., Li-Weber, M., Friedman, S. L., Galle, P. R., Stremmel, W., Oren, M., and Krammer, P. H. p53 activates the CD95 (APO-1/Fas) gene in response to DNA damage by anticancer drugs. J. Exp. Med., *188:* 2033–2045, 1998.
45. Nichols, A. F., Itoh, T., Graham, J. A., Liu, W., Yamaizumi, M., and Linn, S. Human damage-specific DNA-binding protein p48. Characterization of XPE mutations and regulation following UV irradiation. J. Biol. Chem., *275:* 21422–21428, 2000.
46. Kawabata, M., Imamura, T., Inoue, H., Hanai, J., Nishihara, A., Hanyu, A., Takase, M., Ishidou, Y., Udagawa, Y., Oeda, E., Goto, D., Yagi, K., Kato, M., and Miyazono, K. Intracellular signaling of the TGF-β superfamily by Smad proteins. Ann. NY Acad. Sci., *886:* 73–82, 1999.
47. Wang, Y., Rea, T., Bian, J., Gray, S., and Sun, Y. Identification of the genes responsive to etoposide-induced apoptosis: application of DNA chip technology. FEBS Lett., *445:* 269–273, 1999.